18TH WORLD CONFERENCE ON EARTHQUAKE ENGINEERING
WCEE2024
MILAN

MILAN, ITALY
30TH JUNE - 5TH JULY 2024
www.wcee2024.it

EVALUATION OF ENERGY-BASED PARAMETERS REGARDING SEQUENTIAL EARTHQUAKES

M. A. Erberik[1] & F. Gokmen[2]

[1] Professor, Middle East Technical University Civil Engineering Department, Ankara, Turkiye, altug@metu.edu.tr

[2] PhD Candidate, Middle East Technical University Civil Engineering Department, Ankara, Turkiye

Abstract: *Sequential earthquakes are multiple destructive seismic events that can affect population of buildings within a region in a short period of time that is not sufficient to recover from the adverse effects of the disaster between two consecutive events from both engineering and socio-economical points of view. There are many examples of such earthquake sequences in earthquake prone regions of the world in the last few decades. The recent 2023 Kahramanmaras, Turkiye earthquake sequence is one of the most remarkable ones in which four destructive earthquakes with M>6 hit the highly populated south-east region of Turkiye within two weeks. Hence the seismic response of structures under such sequential earthquakes should be examined for state-dependent damage estimation of building populations and management of post-earthquake disaster affairs. For this purpose, this study is focused on the presentation of energy based peak and spectral parameters by employing the selected ground motion records from the 2023 Kahramanmaras, Turkiye earthquake. At the final stage, the obtained results are discussed by putting the emphasis on the revisions required in the conventional seismic design and assessment procedures.*

1. Introduction

Sequential earthquakes are multiple destructive seismic events that can affect population of buildings within a region in a short period of time that is not sufficient to recover from the adverse effects of the disaster between two consecutive events from both engineering and socio-economical points of view. The most important issue is that current seismic design practice considers the seismic action and the corresponding demand from a single event or scenario and the influence of sequential or multiple earthquakes affecting the same structure is not taken into consideration. This issue has been addressed by some researchers in the last two decades and currently more research is being conducted regarding the seismic performance of structures when subjected to earthquake sequences (Hatzigeorgiou and Beskos 2009, Hatzigeorgiou and Liolios 2010, Jeon et al 2015, Manafpour and Moghaddam 2019).

The reason of considering the multiple earthquakes is that there are many examples of such occurrences all over the world in the past. Table 1 presents some of the significant earthquake sequences in the last 25 years. Among these, 2007 Sumatra Indonesia and 2011 Tohoku Japan earthquake sequences are megathrust multiple events with epicentres in the ocean and far away from populated residential areas. Most of the physical and economical losses were due to the triggered tsunami waves that hit the coast rather than the very strong shaking caused by the events with very large magnitude, even exceeding M>8 (Briggs 2007, Lorito *et* al 2008, Zhao 2015). On the other hand, 1999 Chi-Chi Taiwan earthquake sequence occurred on land and in the vicinity

of populated regions of the country, causing structural damage to tens of thousands of buildings with a high death toll.

Table 1. Significant sequential earthquakes in the world in the last 25 years

Date	Location	Magnitude	General Info
20.09.1999	Chi-Chi, Taiwan	7.6	51,700 buildings collapsed and 53,700 were severely damaged. Death toll was 2,415. Generally high-rise buildings with soft/weak stories collapsed (MCEER 2000)
20.09.1999		6.2	
20.09.1999		6.2	
22.09.1999		6.2	
25.09.1999		6.3	
12.09.2007	Sumatra, Indonesia	8.4	It occurred along a tectonic subduction zone (i.e. a megathrust earthquake). Damage and loss were mostly due to tsunami effect. The death toll was 25 (Lorito *et* al. 2008).
12.09.2007		7.9	
13.09.2007		7.0	
09.03.2011	Tohoku, Japan	7.3	During the sequence, 45,000 buildings collapsed and 121,000 were severely damaged (mostly due to tsunami), death toll was 19,750 (mostly due to drowning) (Di Sarno 2013, Abdelnaby and Elnashai 2014).
11.03.2011		9.0	
11.03.2011		7.9	
11.03.2011		7.7	

There are two important earthquake sequences in Turkiye in the last 25 years as seen in Table 2. 1999 Kocaeli and Duzce earthquakes occurred along the North Anatolian Fault Zone of Turkiye within 3 months. The first event affected nearly all Marmara (Northwest of Turkiye) region with a death toll around 15,000 whereas the second event took place in the east of Marmara region with an additional death toll of approximately 3,000. Duzce was the most hardly hit city during these multiple events (Sucuoglu and Yilmaz 2001).

In the 2011 Van Turkiye earthquake sequence, the first event took place in Erciş province of Van city, causing extensive damage to built environment. The third event that took place 2 weeks later caused the collapse of many damaged buildings from the first two events, including a hotel building full of journalists and rescue teams from other countries being trapped under rubble (Erdik *et* al. 2012).

Table 2. Significant sequential earthquakes in Turkiye in the last 25 years

Date	Location	Magnitude	General Info
17.08.1999	Kocaeli / Duzce, Turkiye	7.4	20,000 buildings collapsed and 120,000 were severely damaged. 20 viaduct, 5 tunnels were damaged. Death toll was 18,000 (Sucuoglu and Yilmaz 2001, Spence *et* al. 2003).
12.11.1999		7.1	
23.10.2011	Van, Turkiye	7.3	After the first event, 2,250 buildings collapsed and 6,000 buildings were severely damaged. After the second event, 25 more buildings collapsed in Van. Total death toll was 644 (Erdik *et* al. 2012).
23.10.2011		6.0	
09.11.2011		5.7	

Recently, Turkiye experienced multiple destructive earthquakes in February 2023 as one of the most remarkable earthquake sequences in the world history with four destructive earthquakes having M>6 that hit the highly populated south-east region of Turkiye within two weeks (Table 3). The first two earthquakes (Mw=7.7 and Mw=6.8) occurred in a very short period of time with very close epicentres resembling a multiple segment rupture, therefore it is not easy to make a distinction in between and most of the reliable recorded

ground motion traces belong to the first event. This event, which occurred at night 4:17 a.m. local time, caused the most extensive damage and loss within the earthquake sequence. Then 9 hours later, another destructive earthquake (Mw=7.6) took place with an epicentre at the north east of the epicentres of the first two events. This earthquake knocked down thousands of damaged buildings in the region but the death toll was not that high since it was noon time and most of the people were outside of their houses because of the first event. Finally an earthquake (Mw=6.4) took place two weeks after the first three events with the epicentre in Defne Antakya, which is the most hardly city in this earthquake sequence. This last event also razed down many damaged buildings and the people who had entered to these buildings in order to take their goods were severely injured or killed.

Table 3. Event information related to the 2023 Kahramanmaras Turkiye earthquake sequence

Event	Date	Time (local)	Epicenter	Mw (AFAD)	Depth (km)
E1	6.02.2023	04:17	Pazarcik	7.7	8.6
E2	6.02.2023	04:28	Nurdagi	6.8	6.2
E3	6.02.2023	13:24	Elbistan	7.6	7.0
E4	20.02.2023	20:04	Defne	6.4	21.7

This earthquake sequence is unique from many different aspects: This study focuses on the energy-based intensity parameters of the ground motion records in the selected stations for the 2023 Turkiye earthquake sequence and compares the findings with the ones obtained from the records taken from the previous earthquakes in Turkiye. It also investigates the effect of multiple earthquakes on simple structures by considering the 2023 earthquake sequence as a case study.

2. The 2023 Kahramanmaras Turkiye earthquake sequence

The 2023 Turkiye earthquake sequence occurred on the East Anatolian Fault (EAF), which is one of the major fault systems in Turkiye. As a left-lateral strike slip fault system, it extends from Karlıova in the east to Hatay in the south for a length of approximately 450 km (Saroglu et al., 1992; Westaway, 1994). The EAF zone, in contrast to the North Anatolian Fault (NAF) zone, has been quite and inactive for a considerable period of time (Ambraseys, 1989; Duman and Emre, 2013). The seismic activity in the EAF started in 2010 by the rupture of one of the minor segments of the fault near Karakocan Elazig, causing an earthquake of Mw=6.1 and mainly affecting the rural areas in the region. Then after a decade, there was a rupture in the western segment of the part that caused the 2010 earthquake. Hence an earthquake of Mw=6.7 that had an epicentre in Sivrice town near Elazig city affected the region once more in 2020. These two earthquakes were considered as evidences of a propagation of the EAF in the southwest direction.

The expectations were unfortunately realized on February 6, 2023 as the adjacent segments of the EAF to the southwest direction started to rupture. As it can be seen in Figure 1, the first event (E1 in Table 3) took place at 4:17 am that started at a minor branch of the EAF and then jumped to the main fault line and ruptured multiple fault segments in different directions (yellow lines in Figure 1). The E1 event was a great earthquake that ruptured more than 300 km on the fault line and caused lateral surface deformations in the range of 3-7 meters. This event can also be regarded as the one that caused the most extensive damage and loss in most of the affected cities. The second event (E2 in Table 3) occurred 10 minutes later than the E1 event, rupturing one of the secondary faults (red line in Figure 1). The epicentres of the events E1 and E2 are very close to each other (see Figure 1). It is not very possible to distinguish the effect of this earthquake from the E1 event in the disaster area since they happened one after the other. The next event occurred approximately 9 hours later than the first two events that ruptured another fault in the north of the main EAF line (green lines in Figure 1) with an epicentre close to Elbistan province of Kahramanmaras city. The E3 event caused the collapse of many of the damaged buildings during events E1 and E2, increasing the regional seismic damage even more if not the physical losses. Since events E1-E3 happened in a very short duration of time, there was no time to show any kind of reaction to these events in terms of post-disaster management and relief. Finally, 2 weeks

later, while the rescue teams were still searching thousands of rubbles for possible trapped lives, the fourth event took place close to the south end of the rupture in the E1 event. This was a local event with an epicentre in Defne, Antakya and mainly affected the areas near Hatay city in Turkiye (blue line in Figure 1). There are tens of thousands of aftershocks after the E1 event in the area in the recent months but only these 4 events have been chosen in this study due to their high magnitude (M>6) and damageability potential.

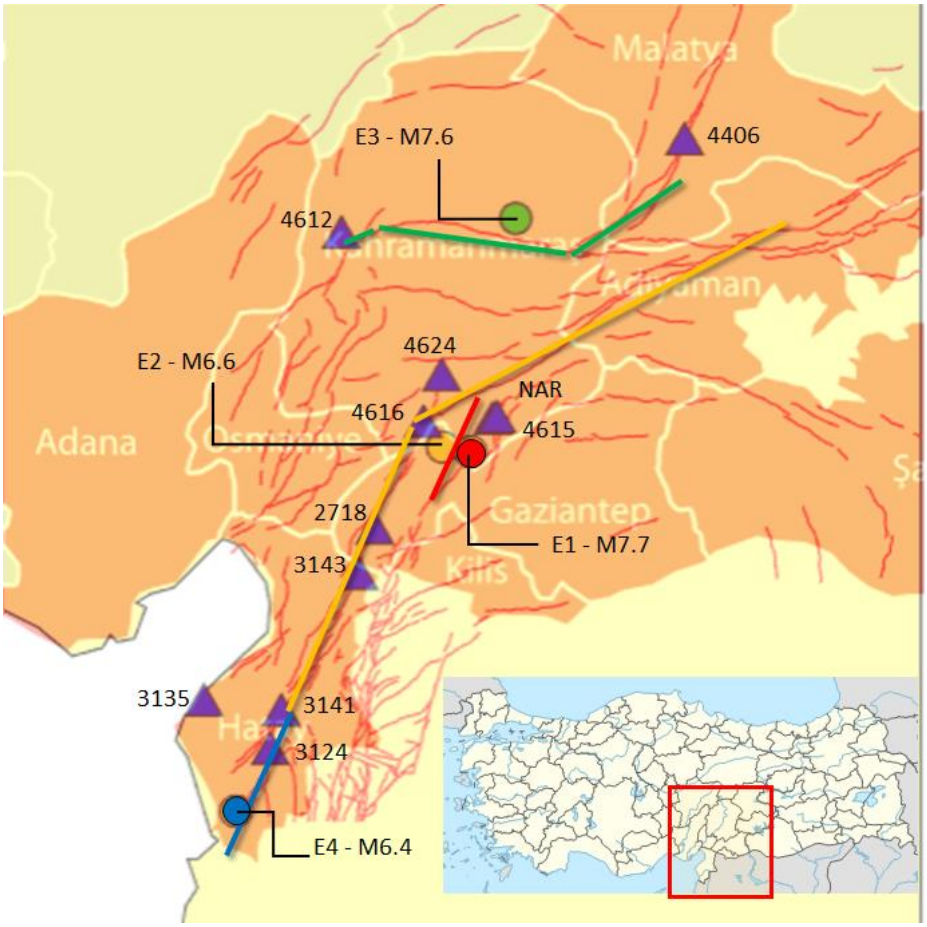

Figure 1. Simple sketch indicating the epicentres and the fault ruptures during the selected events.

There exist many strong motion stations in the affected region that have been operated by AFAD (Disaster and Emergency Presidency of Turkiye). The related raw and filtered strong motion data of the considered events can be downloaded from the AFAD website (https://tadas.afad.gov.tr/). Among tens of stations, 11 of them are selected in this study to investigate the effect of energy related parameters under the 2023 Turkiye earthquake sequence (shown as purple triangles in Figure 1). The main properties of the selected stations are presented in Table 4 (AFAD 2023).

The elastic response spectra of events E1-E4 are presented in Figure 2 for some selected stations (i.e. 2718, 3124, 3135, 4406) together with the elastic design spectra having return periods of 475 years (design-basis earthquake, DBE) and 2475 years (maximum credible earthquake, MCE) as dictated by the latest Turkish seismic code (TBSC 2018). The plots reveal that the spectral design values are exceeded at some specific periods, also depending on the distance between the locations and epicentres of the events. For instance, in station 2718, event E1 seems to be comparable to the DBE whereas the other events have lower spectral values. At longer periods (T>1.5 seconds), it is also comparable to the MCE, verifying why so many mid-rise (4-10 stories) RC frame buildings collapsed in Islahiye, Gaziantep during the first event. In station 3124, events E1 and E4 with closest epicentral distances to the station have significantly higher spectral acceleration values than the design values within wide period ranges (between 0.5 seconds and 2.3 seconds for the DBE and between 0.7 seconds and 1.5 seconds for the MCE), explaining why thousands of buildings in Antakya, Hatay with fundamental periods within the given ranges collapsed in few minutes during event E1 and the remaining

damaged buildings in the same region were razed down two weeks later during event E4. The trends for station 3135 indicate that low-rise buildings with shorter periods (T<1 seconds) could have been affected from events E1 and E4 due to amplified spectral accelerations compared to the corresponding design values. In both stations, events E2 and E3 have very low spectral acceleration values. Finally, in station 4405, only event E3 is comparable to the DBE in the whole period range and E1 in the relatively long period range (T>1.2 seconds) since this station is close to these two events. Overall, it can be stated that the sequential events had different effects on the built environment, which is consistent with the observed damage.

Table 4. Main properties of the selected strong motion stations in the earthquake affected region

Station ID	Province	District	Latitude	Longitude	Altitude (m)	Vs30 (m/s)
2718	Gaziantep	Islahiye	37.008	36.627	527	-
3124	Hatay	Antakya	36.239	36.172	84	283
3135	Hatay	Arsuz	36.409	35.883	3	460
3141	Hatay	Antakya	36.373	36.220	111	338
3143	Hatay	Hassa	36.849	36.557	430	444
4406	Malatya	Akcadag	38.344	37.974	1050	815
4612	Kahramanmaras	Goksun	38.024	36.482	1340	246
4615	Kahramanmaras	Pazarcik	37.387	37.138	581	484
4616	Kahramanmaras	Turkoglu	37.375	36.838	499	390
4624	Kahramanmaras	Onikisubat	37.536	36.918	466	280
NAR	Kahramanmaras	Narli	37.392	37.157	650	-

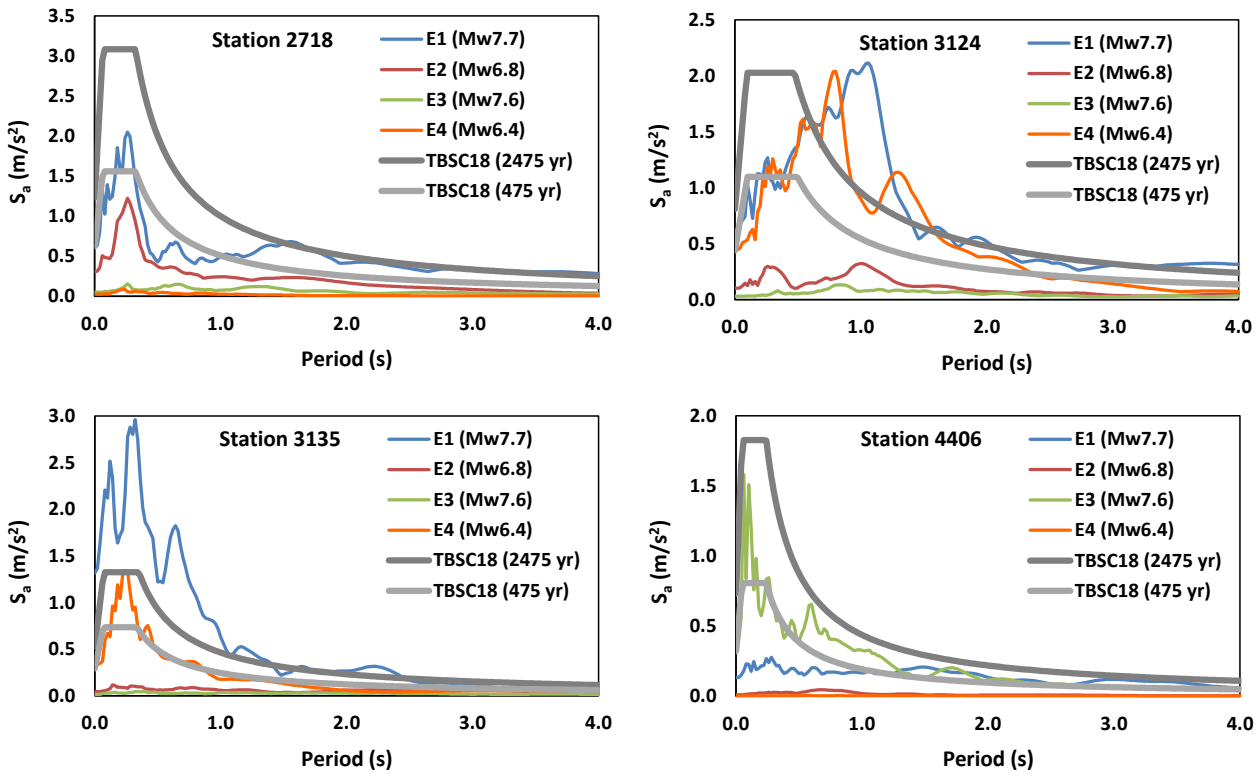

Figure 2. Comparison of elastic response spectra from selected stations with code design spectra.

3. Energy-related Parameters Obtained from the Selected Records

This section focuses on the energy-based parameters of the ground motion records from the selected stations in Table 4. The considered records are among the most extraordinary time-histories ever recorded during the major earthquakes in the last decades. The related ground motion intensity parameters of the time-histories that had been recorded during the 2023 Turkiye earthquakes are being assessed by many researchers. This study considers only the energy-based intensity parameters in order to evaluate the damage potentials of the 2023 earthquakes. The ground motion intensity parameters can be directly obtained from 1) the peak instrumental values, 2) integration of ground motion records in the time domain, 3) frequency content, 4) demand obtained through dynamic analysis of single degree of freedom (SDoF) systems subjected to the considered time-histories. In this study, the following parameters have been evaluated as energy-related measures (see Table 5): peak ground velocity (PGV), Arias Intensity (I_A) (Arias 1970), root-mean-square acceleration in total duration (a_{rms}), cumulative absolute velocity (CAV) (Campbell and Bozorgnia 2012), effective duration (t_{eff}) (Trifunac and Brady 1975), Housner intensity (I_H) (Housner 1952) and input energy intensity (I_E) (Sucuoglu *et* al. 1999). The velocity and duration related terms have also been considered since energy is known to have a direct relationship with these two quantities (Mollaioli *et* al. 2019, Chen *et* al. 2023).

Table 5. Energy-related parameters considered in this study

Station	Event	Dist. (km)	PGV (m/s)	t_{eff} (s)	I_A (m/s)	a_{rms} (10^{-1}·g)	CAV (g·s)	HI (g·s^2)	EI (m/s)
2718	E1	48.3	1.13	20.8	4.25	0.615	2.24	0.254	2.34
	E2	42.0	0.33	5.2	0.62	0.196	0.52	0.115	0.32
	E3	131.8	0.14	30.8	0.06	0.058	0.35	0.034	0.29
	E4	110.3	0.02	22.7	0.01	0.019	0.10	0.008	0.03
4615	E1	13.8	1.28	47.1	5.95	0.607	3.22	0.303	2.00
	E2	21.4	0.20	17.0	0.17	0.102	0.44	0.078	0.21
	E3	78.6	0.29	39.7	0.13	0.088	0.54	0.035	0.29
	E4	169.7	0.02	42.3	0.00	0.010	0.07	0.006	0.02
4616	E1	20.5	0.84	41.0	3.77	0.483	2.50	0.214	0.95
	E2	10.7	0.22	8.2	0.44	0.166	0.52	0.103	0.15
	E3	86.8	0.13	35.7	0.09	0.074	0.43	0.019	0.17
	E4	155.2	0.01	32.0	0.00	0.010	0.07	0.004	0.02
NAR	E1	15.4	0.93	42.6	3.33	0.454	2.30	0.214	2.04
	E2	23.1	0.10	16.4	0.10	0.099	0.33	0.041	0.15
	E3	77.8	0.25	32.3	0.10	0.077	0.38	0.020	0.22
	E4	171.1	0.01	47.7	0.00	0.006	0.04	0.003	0.02
4624	E1	29.7	0.61	45.5	4.33	0.517	2.90	0.217	0.99
	E2	25.8	0.12	17.1	0.28	0.133	0.56	0.067	0.13
	E3	67.7	0.18	45.4	0.25	0.124	0.76	0.049	0.62
	E4	174.3	0.02	34.8	0.01	0.017	0.11	0.009	0.03
4612	E1	95.6	0.14	50.7	1.23	0.267	1.85	0.074	0.26
	E2	88.9	0.07	28.4	0.14	0.089	0.49	0.034	0.06
	E3	66.7	0.73	25.9	3.19	0.444	1.95	0.336	1.04
	E4	214.7	0.02	41.0	0.01	0.016	0.12	0.008	0.02
4406	E1	143.07	0.27	40.6	0.32	0.129	0.81	0.072	0.71
	E2	148.11	0.01	36.3	0.00	0.013	0.09	0.007	0.02
	E3	70.17	0.35	17.5	2.67	0.406	1.72	0.109	0.38
	E4	298.95	0.00	76.9	0.00	0.002	0.01	0.001	0.01
3135	E1	142.15	0.65	22.6	6.77	0.593	2.87	0.289	0.63
	E2	135.71	0.09	39.9	0.04	0.046	0.29	0.028	0.32
	E3	222.04	0.09	87.7	0.02	0.030	0.29	0.014	0.21
	E4	36.30	0.25	8.4	1.31	0.285	0.98	0.092	0.35

Table 5 (cont'd). Energy-related parameters considered in this study

Station	Event	Dist. (km)	PGV (m/s)	t_{eff} (s)	I_A (m/s)	a_{rms} (10^{-1}·g)	CAV (g·s)	I_H (g·s^2)	I_E (m/s)
3124	E1	140.11	0.97	18.9	7.71	0.633	3.37	0.402	2.38
	E2	135.90	0.14	79.9	0.20	0.102	0.64	0.062	0.47
	E3	226.42	0.12	57.3	0.07	0.054	0.47	0.032	0.38
	E4	26.22	0.76	10.2	4.59	0.533	1.85	0.374	0.80
3141	E1	125.42	1.24	13.3	15.15	0.887	4.34	0.413	1.86
	E2	120.87	0.06	31.6	0.08	0.065	0.38	0.032	0.20
	E3	211.11	0.10	60.8	0.02	0.033	0.28	0.015	0.16
	E4	41.36	0.15	12.3	0.91	0.237	0.92	0.063	0.10
3143	E1	65.13	1.04	26.4	2.48	0.391	1.88	0.242	1.46
	E2	59.98	0.17	8.6	0.17	0.101	0.35	0.056	0.13
	E3	150.45	0.11	30.0	0.06	0.054	0.35	0.028	0.22
	E4	102.23	0.02	28.1	0.01	0.017	0.10	0.007	0.03

The formulations of the considered parameters can be presented as follows:

(Arias Intensity, I_A) $$I_A = \frac{\pi}{2g}\int_0^{t_d}\left[\ddot{u}_g(t)\right]^2 dt \quad (1)$$

(Root mean acceleration, a_{rms}) $$a_{rms} = \sqrt{\frac{1}{t_d}\int_0^{t_d}\left[\ddot{u}_g(t)\right]^2 dt} \quad (2)$$

(cumulative absolute velocity, CAV) $$\mathrm{CAV} = \int_0^{t_d}\left|\ddot{u}_g(t)\right| dt \quad (3)$$

(Housner spectrum intensity, I_H) $$I_H = \int_{0.1}^{2.5} PS_v\, dT \quad (4)$$

(Input energy intensity, I_E) $$I_E = \frac{1}{T}\int_0^{T} v_{eq}\, dT \quad (5.a)$$

where $$v_{eq} = \sqrt{\frac{2E_I}{m}} \quad (5.b)$$

In the above equations, $\ddot{u}_g$ is the ground acceleration, t_d is the total duration of earthquake, *PSv* is the 5% damped pseudo spectral velocity, v_{eq} is the input energy equivalent velocity and E_I is the input energy. Effective duration can be defined as the duration between the instants when I_A reaches the 5% and 95% of its final value. It is regarded as the duration of ground motion that contributes to the damaging part of the seismic response for SDoF systems.

The values calculated for the energy related parameters in Table 5 reveal that there are very high PGV values (i.e. PGV>1m/s) at different stations during the event E1 although the stations are far enough from the epicentre of the event (distance>20 km). In addition, the strong motion durations are quite long for most of the events and stations (t_{eff}>20 s). All the other energy-related parameters in Table 5 verify the damage potential of event E1 except stations 4406 and 4612 for which event E3 is more critical and station 3124 for which event E4 has comparable parameter values when compared to event E1. These trends show the importance of station location and distance from the fault rupture line regarding the repetitive large seismic demands during destructive sequential earthquakes affecting a wide area. Most of the records in Table 5 prove the dominance of event E1 in terms of damage potential to built environment. However, the built environment in the earthquake-hit area also seems to have been affected from the events E3 and E4, depending on the relative locations of the residential area and earthquake epicentre. The latter seems to be more damageable for building stock in the region since the damaged structures in event E1 experience another comparably destructive event in a short period of time.

More information can be obtained by spectral energy values. The most suitable parameter is the input energy that can be obtained by taking the integral of the equation of motion with respect to relative displacement (u) as

$$\int_0^u m\ddot{u}\,du + \int_0^u c\dot{u}du + \int_0^u f_s du = -\int_0^u m\ddot{u}_g du \tag{6}$$

where m is the mass, c is the damping constant and f_s is the restoring force of a typical SDoF system. The term on the right-hand side of Equation 6 is defined as the input energy (E_I), which is an enhanced parameter that is obtained by the convolution of ground motion and structural response parameters. Input energy is known to be very stable since it does not show drastic changes in cases of elastic/inelastic behaviour and variations in damping properties. The spectral plots of E_I are presented for stations 4612, 4624, 4406 and 3124 by considering the cases of single event E1 and sequential events (E1+E2, E1+E2+E3 and E1+E2+E3+E4). Plots reveal different trends of energy input to the structures for different stations. For instance, the structures in the close vicinity of station 4612 seems to have experienced the highest E_I demand during event E3, especially in the period range 1.3 s<T<2.0 s, indicating that the already damaged mid-rise and high-rise flexible buildings during the first two events encountered the most severe energy demand in the third one. In case of the other station in Kahramanmaras province (i.e. station 4624), event E1 possesses the highest energy demand and the other events show minor contributions to input energy demand, especially for long-period structures (i.e. T>2 s). For the station in Malatya province (i.e. station 4406), the dominance of event E3 is observed just like station 4612. However, in this case there is a significant increase of input energy in all the period range, meaning that all the structures have been affected by this increased demand in an adverse manner. Finally for the station in Antakya, Hatay (i.e. 3124), it can be stated that there is an enormous energy input in a narrow period range (i.e. 0.9 s<T<1.2 s) during event E1, nearly no contribution from events E2 and E3, but then another increase in input energy, especially in the vicinity of the amplified spectral values during event E1.

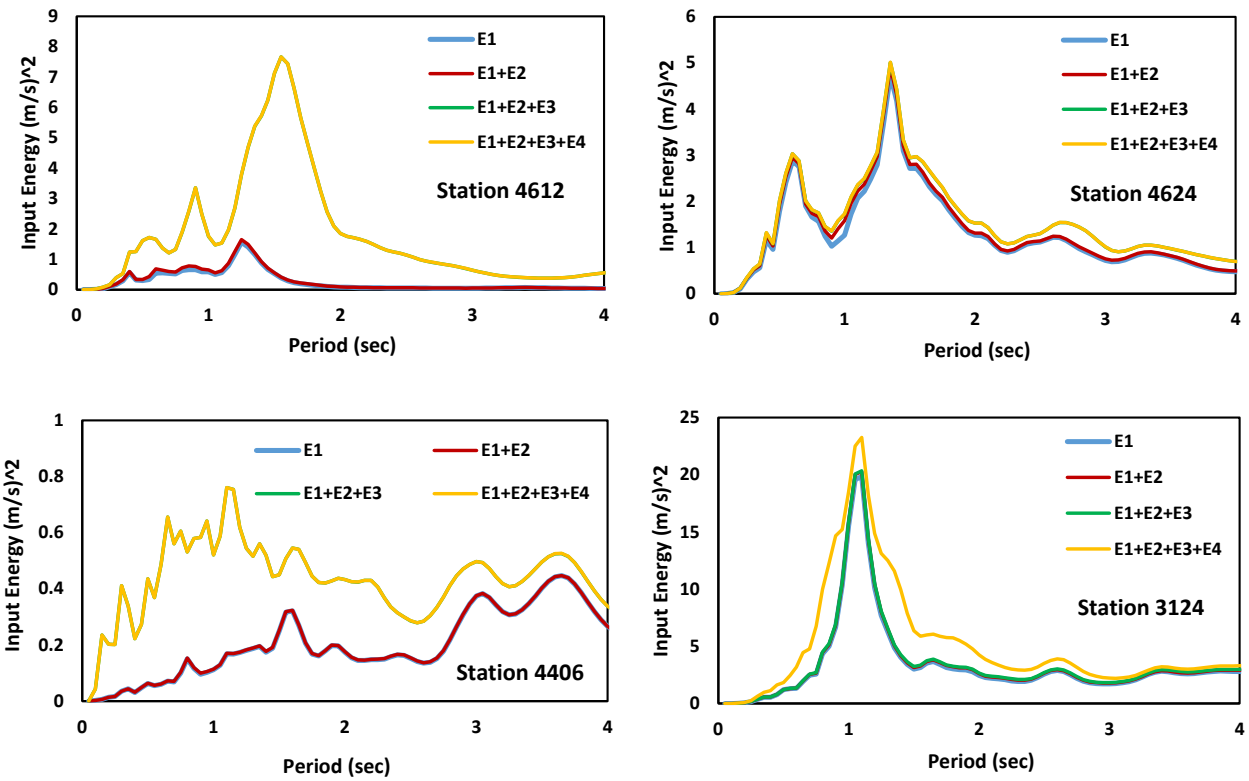

Figure 3. Spectral variation of input energy under sequential events for the selected stations

4. Conclusions

The recent 2023 Kahramanmaras Turkiye earthquake sequence is one of the most remarkable disasters in the world, in which four destructive earthquakes with M>6 hit the highly populated south-east region of Turkiye within two weeks. Hence it is essential to assess the seismic damage potential of the 2023 sequential earthquakes in order to utilize the obtained data for the damage and loss mitigation of future destructive earthquakes. Accordingly, this study is focused on the presentation of energy-based peak and spectral parameters by employing the selected ground motion records from the 2023 Kahramanmaras Turkiye earthquake. The considered peak parameters can be listed as peak ground velocity, Arias Intensity, root-mean-square acceleration, cumulative absolute velocity, effective duration, Housner intensity and input energy intensity. The calculated values of these parameters reveal that event E1 is the most damageable one among the other events for most of the selected stations, however there are also some cases where more than one event (especially events E3 and E4) can be destructive for the built environment in addition to event E1. This can be critical since none of the seismic building codes in the world take into consideration multiple earthquakes taking place in a short period of time. The results also point out the importance of station location and distance from the fault rupture line. Moreover, the input energy spectra of the selected ground motion records reveal that significant levels of energy input can affect the building structures in a wide period range during different events, depending on the relative distance between the location of the building stock and the epicentre of the event. Especially, the medium periods (0.7 s<T< 1.4s) seem to have been highly affected by the amplified energy demands. These periods correspond to flexible mid-rise and high-rise reinforced concrete building structures in the region, which showed a very inferior performance during the 2023 earthquake sequence and thousands of these buildings experienced severe damage or collapse. Overall, from the results it is evident that the energy-based parameters verify the high damage potential of the 2023 sequential earthquakes just like force-based and displacement-based parameters and it is crucial to take some measures in the next generation codes regarding sequential earthquakes and state-dependent performance of structures.

5. References

Abdelnaby, A.E., Elnashai, A. S. 2014. Performance of Degrading Reinforced Concrete Frame Systems under the Tohoku and Christchurch Earthquake Sequences. Journal of Earthquake Engineering 18:1009–1036.

AFAD (2023). 06 February 2023 Pazarcik-Elbistan Kahramanmaras (Mw7.7–Mw 7.6) Earthquakes: Technical Report. Prepared by the Earthquake and Risk Reduction General Directorate, Republic of Turkey, Ministry on Interior, Disaster and Emergency Management Authority, Ankara, Turkiye.

Ambraseys, N.N., 1989. Temporary seismic quiescence: SE Turkey. Geophysical Journal International, 96(2), 311–331.

Arias, A. 1970. A measure of earthquake intensity. Seismic Design for Nuclear Power Plants, ed. R.J. Hansen. Massachusetts Institute of Technology Press, Cambridge USA, 438-469.

Briggs, R., 2007. Learning from Earthquakes: 2007 Sumatra, Indonesia, Earthquakes. EERI Newsletter 41 (10), page 2.

Campbell, K.W., Bozorgnia, Y. 2012. Cumulative absolute velocity (CAV) and seismic intensity based on the PEER-NGA database. Earthquake Spectra 28(2), 457–485.

Chen G., Yang J., Liu Y., Kitahara T., Beer, M. 2023. An energy-frequency parameter for earthquake ground motion intensity measure. Earthquake Engng Struct Dyn. 52, 271–284.

Di Sarno, L., 2013. Effects of multiple earthquakes on inelastic structural response. Engineering Structures 56, 673–681.

Duman, T.Y., Emre, Ö., 2013. The East Anatolian Fault: Geometry, segmentation and jog characteristics. Geol. Soc. Spec. Publ., 372, 495–529. doi:10.1144/SP372.14.

Erdik, M., Kamer Y., Demircioglu, M., Sesetyan, K., 2012. 23 October 2011 Van (Turkey) earthquake. Natural Hazards 64, 651–665.

Hatzigeorgiou, G. D., Beskos, D. E., 2009. Inelastic displacement ratios for SDOF structures subjected to repeated earthquakes. Engineering Structures 31, 27442755.

Hatzigeorgiou, G. D., Liolios, A. A., 2010. Nonlinear behaviour of RC frames under repeated strong ground motions. Soil Dynamics and Earthquake Engineering 30, 1010–1025.

Housner, G.W. Spectrum intensities of strong motion earthquakes. Proceedings of the Earthquake and Blast Effects on Structures Symposium, EERI, Los Angeles, USA, 21-36.

Jeon, J.S., Des Roches, R., Lowes, L. N., Brilakis, I., 2015. Framework of aftershock fragility assessment–case studies: older California reinforced concrete building frames. Earthquake Engng Struct. Dyn. 44, 2617–2636.

Lorito, S., Romano, F., Piatanesi, A., Boschi, E. 2008. Source process of the September 12, 2007, MW 8.4 southern Sumatra earthquake from tsunami tide gauge record inversion. Geophysical Research Letters. 35 (2), L02310. doi:10.1029/2007GL032661.

Manafpour, A. R., Moghaddam, P. K. 2019. Performance capacity of damaged RC SDOF systems under multiple far- and near-field earthquakes. Soil Dynamics and Earthquake Engineering 116, 164–173.

Mollaioli, F. Donaire-Avila, J. Lucchini, A., Benavent-Climent A. On the importance of energy-based parameters. ECCOMAS Proceedia COMPDYN, 2244-2270.

Multidisciplinary Center for Earthquake Engineering Research (MCEER) 2000. The Chi-Chi, Taiwan Earthquake of September 21, 1999: Reconnaissance Report. Edited by: Lee, G.C. and Loh, C. H. Technical Report MCEER-00-0003, University at Buffalo, State University of New York, USA.

Saroglu, F., Emre, Ö., Kuscu, İ. (1992) The East Anatolian Fault zone of Turkey. Ann.Tecton., 6,99-125 (Special Issue-Supplement).

Spence, R., Bommer, J., Del Re, D., Bird, J., Aydinoglu, N., Tabuchi, S., 2003. Comparing Loss Estimation with Observed Damage: A Study of the 1999 Kocaeli Earthquake in Turkey. Bulletin of Earthquake Engineering 1, 83–113.

Sucuoglu, H., Gulkan, P., Erberik, A., Akkar, S. 1999. Measures of ground motion intensity in seismic design. Proceedings of the Ugur Ersoy Symposium on Structural Engineering, Middle East Technical University, Ankara, Turkiye, 105-121.

Sucuoglu, H., Yilmaz, T., 2001. Duzce, Turkey: A City Hit by Two Major Earthquakes in 1999 within Three Months. Seismological Research Letters 72(6), 679-689.

Trifunac, M.D., Brady, A.G. 1975. A study on the duration of strong earthquake ground motion. Bulletin of the Seismological Society of America 65(3), 581-626.

Westaway, R. (1994). Present-day kinematics of the Middle East and eastern Mediterranean. J. Geophys. Res., 99, 12071-12090.

Zhao, D. (2015). The 2011 Tohoku earthquake (Mw 9.0) sequence and subduction dynamics in Western Pacific and East Asia. Journal of Asian Earth Sciences 98, 26–49.